Systematic Analysis and Model Interpretation of Micromolecular Non-Fickian Sorption Kinetics in Polymer Films

M. Sanopoulou and J. H. Petropoulos*

Physical Chemistry Institute, Demokritos National Research Centre, GR-15310 Aghia Paraskevi, Athens, Greece

Received August 10, 1998; Revised Manuscript Received November 14, 2000

ABSTRACT: This paper confirms and amplifies our previous demonstration (Sanopoulou, M.; Roussis, P. P.; Petropoulos, J. H. *J. Polym. Sci.: Part B: Polym. Phys.* **1995**, *33*, 993) that suitable systematic analysis and model interpretation of various features of weight gain (and loss) kinetic data, can lead to significant unambiguous conclusions concerning the physical nature and cause(s) of non-Fickian (NF) organic vapor sorption in polymer films. The relevant NF kinetic features, the modeling approaches used to provide the requisite theoretical background for analysis of the said NF features and the conclusions which can be drawn, are discussed in some detail. We then present, with the aid of supplementary new data, a much more detailed analysis and model interpretation of NF sorption in the cellulose acetate−acetone system than was given in our previous work cited above, and discuss the implications of the results obtained with regard to current views concerning the NF behavior of polymer−penetrant systems in general.

Introduction

According to Crank,[1,2] non-Fickian (NF) sorption kinetics in polymer film−organic vapor systems is physically attributable to (a) the viscoelastic nature of the polymer and, in particular, to slow viscous structural relaxation of the swelling or deswelling polymer and/or (b) the differential swelling stresses (DSS) generated by the constraints imposed on local swelling (deswelling) by the less (more) swollen regions of the polymer sample during the sorption experiment.

Effects a and b, of course, coexist, but in view of the complexity of a comprehensive approach, they were treated by Crank[2] separately, in terms of what may conveniently be referred to as the "volume viscous relaxation" (VVR) and "differential swelling stress" (DSS) model approaches, respectively.

Crank[2] gave equal attention to each of these approaches, a policy subsequently adopted in our own modeling work too (see below). However, experimental NF sorption data have, so far, been widely interpreted in terms of viscous relaxation phenomena, paying scant attention to the possibility of significant DSS-induced deviations from Fickian behavior (see below).

Accordingly, in a recent paper,[3] concerned with a detailed study of sorption kinetics in the cellulose acetate (CA)−acetone vapor system, we (i) stressed the importance of identifying the physical cause(s) of observed NF behavior, before engaging in detailed model interpretation thereof; (ii) indicated that this could be accomplished in a systematic manner by suitable kinetic analysis of the sorption data; and (iii) presented a practical demonstration of such analysis. The results obtained revealed the presence of significant DSS effects over a wide range of conditions and enabled us to identify a common type of NF sorption behavior as purely DSS-induced. A companion paper[4] served to demonstrate the kind of supplementary or confirmatory information that may be obtained by performing parallel longitudinal swelling (LS) measurements and correlating the results with the corresponding sorption data.

In a subsequent paper by Samus and Rossi[5] (SR), kinetic data on liquid methanol absorption in ethylene−vinyl alcohol (EVA) copolymers were reported and (correctly) interpreted (with the aid of corresponding LS data) as purely DSS-induced. These authors also embarked on an extensive review of previous approaches to the model interpretation of NF sorption kinetics, with which it is difficult to agree fully (see below). We have taken particular note of what is, in our opinion, an unduly pessimistic view of the physical insight into NF kinetic behavior which may be gained from sorption (weight gain or loss) experiments.[5]

Sorption experiments, as normally performed, involve effectively unidimensional diffusion of a micromolecular penetrant in a thin polymer film with surfaces maintained at constant penetrant activity a_F. The film is initially equilibrated with a different penetrant activity a_I (where $a_I < a_F$ in absorption and $a_I > a_F$ in desorption). We designate by Q_t and Q_∞ penetrant uptake or loss per unit (dry) film area at time t and at $t \rightarrow \infty$, respectively. The latter condition denotes the establishment of final equilibrium at a_F. Thus, $Q_\infty = 2l|C_F - C_I| = 2l\Delta C$; where C_I and C_F represent the initial and final (uniform) concentrations of sorbed penetrant in the polymer film respectively (given here in g of penetrant per cm^3 of pure polymer; the resulting numerical values of C turn out to be only a little lower than those of the corresponding volume fraction of penetrant in the swollen film), and l is the half thickness of the pure polymer film.

Fickian kinetics is essentially characterized by experimental Q_t/Q_∞ vs $t^{1/2}/l$ plots which (a) exhibit a substantial initial linear portion passing through the origin and (b) are independent of l for a given set of experimental conditions. Note that the initial linearity in Q_t vs $t^{1/2}$ should persist, as long as the polymer film behaves as an effectively semiinfinite medium. For practical purposes, this is so up to $Q_t/Q_\infty \sim 0.5$ for a

* To whom correspondence should be sent. Telephone: +30-1-6503787, +30-1-6503785. Fax: +30-1-6511766. E-mail: petrop@mail.demokritos.gr; sanopoul@mail.demokritos.gr.

10.1021/ma981255o CCC: $20.00
Published on Web 01/24/2001

polymer film-penetrant system characterized by constant diffusivity D.[6a] Note also that we designate as "non-Fickian" behavior all deviations from normal Fickian sorption kinetics not attributable to imperfect experimental design.

SR rightly point out that mere deviation from the aforementioned Fickian criterion (a) (most commonly in the form of S-shaped absorption Q_t vs $t^{1/2}$ curves) cannot be given an unequivocal physical interpretation, a point already shown by Crank[2] and further emphasized in our own modeling work (see below). Furthermore, the aforementioned paper of ours[3] was intended to demonstrate the resolution *in practice* of ambiguities of precisely this kind, by the method of systematic analysis outlined therein. Here, we proceed to a full discussion of this method and its application. Accordingly, in the next section, we begin by noting the main features of NF sorption kinetics commonly encountered in practice. We then proceed to describe, and justify our choice of, the approaches used to provide the theoretical background for analysis and model interpretation of the aforementioned NF features. In a subsequent section, we describe the general patterns of NF absorption behavior brought to light by systematic experimental studies, involving series of so-called "interval" or "integral" sorption experiments. Finally, we proceed, with the aid of a more complete set of data, to a much more detailed, in depth analysis and model interpretation of the NF sorption behavior exhibited by the CA−acetone system than was possible in ref 3.

Model Interpretation of NF Sorption Behavior

A list of characteristic deviations from Fickian sorption behavior *commonly* observed (i.e., excluding such unusual system-specific features as "sorption overshoots") includes the following:[1−3,6b−12] (1) S-shaped absorption Q_t/Q_∞ vs $t^{1/2}$ curves, which initially lie below and then cross the corresponding (convex upward) desorption ones; (2) "two-stage" Q_t vs $t^{1/2}$ curves; (3) Q_t/Q_∞ vs $t^{1/2}/l$ plots not independent of l, under otherwise identical experimental conditions; (4) cases of feature 1 where the amount Q_t absorbed by a thinner film initially exceeds that taken up by a thicker one, under otherwise identical experimental conditions; (5) cases of feature 1, where Q_t in the absorption mode turns out to be linear when plotted on a t scale and the formation of sharp penetration fronts is an additional characteristic feature ("case II" kinetics); (6) cases of feature 1 where Q_t in the absorption mode remains in part concave upward when plotted vs t ("super case II" kinetics).

We describe here briefly the main approaches used for model interpretation of NF sorption data.

Volume Viscous Relaxation (VVR) Modeling Approach.[2,3,6b,7,8,13−26] In this approach, the effect of viscous relaxation is treated in a simplified manner, by considering the temporal evolution of the overall degree of penetrant-induced swelling of any given volume element in a viscoelastic polymer sample, without regard to any constraints imposed by the swelling behavior of other volume elements (i.e., neglecting DSS effects). Swelling of the polymer (under a penetrant-induced "osmotic stress")[14,27,28] is treated (in close analogy with viscoelastic deformation under mechanical stress) as consisting of an "instantaneous" ("elastic") component plus a "delayed" ("viscous") component. The latter component is physically due to molecular relaxations of the polymer closely similar to those seen in mechanical creep (see below), and gives rise to time-dependent solubility (TDS), and possibly time-dependent diffusivity (TDD), of the penetrant in the polymer.

Although TDD-type models have been presented by Crank[2] and some others,[22] most authors have justifiably adopted the TDS-type (usually uncomplicated by TDD) approach, which has the advantage of close physical analogy to the treatment of mechanical viscoelastic deformation.[28] In either case, the time dependence of the local solubility (S) or diffusion (D) coefficient is most simply described as a pseudo-first-order relaxation process governed by an effective rate constant or relaxation frequency (i.e., reciprocal relaxation time) β.

The fact that the viscous relaxation rate does not scale with l^2, as does the diffusion rate (the effective rate constant for which is D/l^2), leads to sorption kinetics which violates both Fickian criteria a and b given above. This NF behavior was discussed by Crank[2] in terms of a "NF modulus" defined as the ratio of the aforementioned effective rate constants (which turns out to be the reciprocal of the more recently introduced Deborah number):[29] $\alpha_R = l^2\beta/D$. More specifically, the VVR modeling approach predicts, for values of α_R which are neither too low nor too high, the occurrence of NF feature 1 in association with feature 3. The TDS version of this approach also predicts NF feature 2 (not explicable in purely TDD terms) at sufficiently low values of α_R. It has been shown[7] experimentally that in two-stage absorption, with clearly separated first and second stages, the first stage represents diffusion into the effectively unrelaxed polymer and terminates with the establishment of a quasiequilibrium characterized by nearly uniform concentration $C_q < C_F$ (with $\Delta C_1 = C_q - C_I$ corresponding to the aforementioned elastic swelling component). The second stage then represents gradual relaxation of this nearly uniform concentration (denoted by C_2); from $C_2 = C_q$ to $C_2 = C_F$ (i.e., the aforementioned viscous swelling component corresponds to $\Delta C_2 = C_F - C_q$) and thus affords the opportunity of studying the rate and kinetics of the TDS phenomenon, under conditions where the model assumption of unconstrained local swelling is indeed valid (because of the absence of significant concentration gradients). In the course of such studies, second-stage absorption relaxation rates were compared with those of mechanical creep and shown to be closely similar[30] (thus providing strong evidence of the close physical correspondence between TDS and mechanical viscoelastic behavior). It was also established[8] that β is generally a function of both C and ΔC.

Differential Swelling Stress (DSS) Modeling Approach.[2,11,18,31−39] This approach involves (i) evaluation of the differential swelling stresses, which develop as a result of the nonuniform distribution of sorbed penetrant in the polymer sample during the sorption experiment (in a manner analogous to thermal stresses generated by uneven heating), coupled with (ii) the consideration that S and D tend to be locally enhanced (reduced) by tensile (compressive) differential swelling stresses or strains.

Crank[2] presented a simplified DSS model, involving strain-dependent diffusivity in a linearly elastic polymeric medium, which was designed to bring out some of the most striking features of NF sorption behavior induced by DSS effects. Subsequent developments[18,31−33,38] have rendered this modeling approach much more realistic (but still open to further elabora-

tion, particularly with regard to the proper simulation of complex viscoelastic behavior) by (i) elimination of the drastic simplifications introduced by Crank[2] for reasons of mathematical convenience; (ii) use of stress-dependent diffusivity or solubility (on the basis of the known effect of stress on polymer fractional free volume[40] or on the chemical potential of sorbed penetrant[35,36] respectively); (iii) extension to the case of a viscoelastic polymeric medium, by the introduction of a simple form of viscous relaxation, namely by allowing viscous relaxation of the DSS governed by a pseudo-first-order rate constant (or relaxation frequency) β_s; and (iv) simplified representation of the effect of nonlinear polymer elasticity or viscoelasticity.

On this basis, the DSS modeling approach can predict NF feature 1 either in association with feature 3 or not, according to whether the polymeric medium exhibits viscoelastic (characterized by finite $\alpha_s = l^2\beta_s/D$ values) or purely elastic (corresponding to either $l^2\beta_s/D \rightarrow 0$ or $l^2\beta_s/D \rightarrow \infty$) behavior. Furthermore, Crank's original identification of NF feature 4 as characteristic of DSS effects[2] has been confirmed under all conditions studied so far by means of the aforementioned more sophisticated versions of this modeling approach. This is largely true also of NF feature 6. On the other hand, NF feature 2 clearly lies beyond the reach of any DSS model, since the absence of appreciable concentration gradients in the second-stage sorption noted above precludes the appearance of significant DSS during that stage.

The usefulness of the DSS modeling approach is enhanced by the fact that it affords the possibility of interpreting the kinetic behavior of the longitudinal swelling or deswelling of the film ($\Delta H_t = |H_t - H_o|$, where H_t denotes the film length at time t), which accompanies the absorption or desorption of penetrant, respectively. The results of such longitudinal swelling (LS) measurements yield significant information about the presence and decay of DSS in the course of the sorption process; and are best considered in correlation with the corresponding sorption data, in the form of $\Delta H_t/\Delta H_\infty$ vs Q_t/Q_∞ plots.[31−33] On the basis of suitable DSS model calculations, a scheme for the systematic analysis and interpretation of such sorption−longitudinal swelling (S−LS) kinetic correlations has been worked out[33] and applied experimentally[4,41] by us.

Model Prediction of NF Feature 5. Although NF feature 5 (special attention to which was drawn by the work of Alfrey et al.)[11] was soon recognized as an extreme form of relaxation controlled absorption kinetics,[42] its appearance could, for a long time, be reproduced theoretically only by postulating the formal presence of a case II convection process occurring simultaneously with normal diffusion.

Various detailed formulations of this "diffusion-with-convection (DwC)" approach, have been proposed.[43−47] In general, the diffusion process may be described in terms of a diffusion coefficient D, which changes from a low value $D = D_1$ (characteristic of unrelaxed polymer), prevailing at or below a certain critical concentration C^*, to a high value $D = D_2 \gg D_1$ (characteristic of relaxed polymer) at $C > C^*$. This type of diffusivity behavior is sufficient to account for the development of a sharp penetration front[6c] separating the relaxed from the unrelaxed polymer region but cannot by itself lead to the constant rate of convection, which is the chief characteristic of case II sorption kinetics. Hence the need for the aforementioned introduction (on what remains up to now an essentially empirical basis) of a convection process governed by velocity v, which is either assumed at the outset to be constant or becomes constant under appropriate conditions.

When applied to the interpretation of NF sorption behavior in general, the DwC approach resembles the VVR one in that it will predict NF absorption feature 1 [desorption, when considered, is erroneously (see below) assumed to be Fickian] in association with feature 3. This follows from the facts that (i) the convection process scales with l (the effective rate constant is v/l) rather than l^2 and (ii) the effect of convection kinetics on the absorption Q_t vs $t^{1/2}$ plot is manifested as a positive deviation from linearity (this tendency is, of course, reversed as final equilibrium is approached, thus giving rise to an S-shaped curve).

An effectively pure case II regime for the duration of the absorption experiment is predicted when (i) $\alpha_{C_2} = vl/D_2 \rightarrow 0$ and (ii) $\alpha_{C_1} = vl/D_1 \rightarrow \infty$. If the former condition is relaxed, the absorption process starts out, in principle, as case II, but then becomes increasingly diffusion-limited (the extent of the observed overall deviation from Fickian kinetics depending on the actual value of $\alpha_{C2} = vl/D_2$; see below). If condition (ii) is relaxed, a low-concentration diffuse Fickian front can build up just ahead of the sharp one, up to a certain limit which corresponds to a maximum penetrant uptake by the Fickian mechanism of $Q_1 = C^*D/v$, under semiinfinite medium conditions.[43] Thus, a case II regime, if observable, will be confined to that portion of the absorption curve where the limit Q_1 has been approached sufficiently closely, on one hand, and the semiinfinite medium condition has not yet been significantly violated on the other hand. Under these or analogous conditions, the resulting Q_t vs $t^{1/2}$ plot should exhibit the characteristics of two-stage absorption and examples have been given of experimental two-stage absorption curves which could formally be reinterpreted in this manner.[48] Such an interpretation of NF feature 2 would, however, be tenable only if accompanied by demonstration of the presence of a case II penetration front; in view of the evidence quoted above that the second stage in two-stage absorption, as it normally occurs in practice, is characterized by practically uniform penetrant concentration across the film. Similarly, there seems to be no possibility of accounting for NF features 4 and 6 in DwC model terms.

Thus, the DwC modeling approach cannot serve as a useful basis for the analysis and interpretation of NF sorption behavior; not only because the appearance of the case II convection process therein lacks a proper physical foundation, but also because important NF kinetic features do not seem to be readily interpretable thereby.

In fact, it is fair to say that this approach lost its *raison d'etre*, when it was shown, more than a decade ago, that case II kinetics lies within the predictive capability of both the aforementioned VVR (TDS version)[19,27] and extended DSS (with stress-dependent solubility coefficient)[34] approaches.

In particular, it is predicted that a case II regime will be spontaneously established (under semiinfinite medium conditions and after an initial induction time), in the course of absorption experiments characterized by (i) a sufficiently large difference of the penetrant solubility in unrelaxed and fully relaxed polymer and

(ii) sufficiently large ΔC to ensure suitably steep changes in D and β (the latter being normally steeper), namely $D(C_F)/D(C_I) \gg 1$, $\beta(C_F)/\beta(C_1) \gg > 1$ and (iii) $l^2\beta(C_I)/D(C_F) \ll 1$(and similarly for β_s in the DSS model). A sharp penetration front, separating nearly fully swollen, relaxed polymer from weakly swollen, unrelaxed (or slowly relaxing) polymer, is generated. This is due to the highly nonlinear autocatalytic nature of the swelling relaxation process (analogous to yielding in the case of mechanical deformation experiments), which ensures that a large part of the resulting local increase in swelling occurs practically instantaneously (in the absence of diffusion limitations), yielding $C \approx C_F$ on the upstream side of the sharp penetration front. On the other hand, the overall relaxation process is rate controlled by the low values of $\beta = \beta(C \rightarrow C_I)$ prevailing in the unrelaxed/slowly relaxing polymer region. The condition $l^2\beta(C_I)/D(C_F) \rightarrow 0$ then ensures absence of diffusion limitations (and hence a flat concentration profile in the relaxed polymer region), so that the sharp front advances at a rate controlled by $\beta(C \rightarrow C_I)$. Model calculations show[19,24,27,34,49] that (apart from an initial induction period) the resulting penetration rate, under semiinfinite medium conditions, is constant in time. Note, incidentally, that a low-concentration diffuse profile preceding the sharp front [the extent of which chiefly depends on $l^2\beta(C_I)/D(C_I)$] is also duly predicted, by virtue of the fact that only relatively minor deviation from Fickian diffusion, with nearly constant $D \approx D(C \rightarrow C_I)$, occurs in the slowly relaxing polymer region.

Diagnostic Criteria of the Physical Origin of Observed NF Kinetic Features. The above discussion indicates that a useful analysis and interpretation of observed NF sorption behavior can be based on the VVR and DSS (treated as complementary rather than mutually exclusive) modeling approaches and leads to the formulation of certain unambiguous diagnostic criteria regarding the underlying physical causes of the said NF behavior. In particular: (i) NF feature 3 emerges as the key criterion indicating the presence of viscous relaxation phenomena, independently of the appearance of significant DSS effects; while NF feature 2 reveals the occurrence of viscous relaxation in the absence of DSS; (ii) NF feature 1 *not* in association with feature 3 implies the presence of DSS, in the absence of viscous relaxation, effects; while NF features 4 and 6 point to DSS, independently of the simultaneous presence of viscous relaxation, effects.

Significance of the NF Modulus. Before closing this section, it is important to dispel possible misconceptions[5] concerning the significance of the NF moduli defined here, following Crank,[2] as $\alpha_R = l^2\beta/D$, $\alpha_s = l^2\beta_s/D$, and $\alpha_c = vl/D$. These moduli provide useful guidance concerning the possible appearance of significant deviations from Fickian kinetics in sorption experiments of the type described above, i.e., in experiments involving diffusion across films of *finite* thickness. However, the parameter l obviously becomes irrelevant in experiments where the polymer substrate behaves throughout as a semiinfinite diffusion medium (as is typically the case in studies of micromolecular penetration *along* the polymer film).[50] As has been pointed out in previous papers,[34,50] the proper NF modulus for such cases is obtained by replacing l in the above definition by an appropriately defined maximum distance of penetration X_∞. Obviously, one may similarly characterize the kinetic regime prevailing at any earlier stage of such an experiment by a NF modulus α_X defined in terms of the appropriate penetration distance X.

As an example, we return to our previous description of the behavior predicted by the DwC model for finite α_{C_2}. The expectation that the absorption process will start out as case II follows from the fact that the requisite condition is initially satisfied (by definition) for finite v/D_2, since $\alpha_{C2X} = vX/D_2 \rightarrow 0$ for $X \rightarrow 0$. On the other hand, l sets the upper limit to X, so the value of $\alpha_{C2} = \alpha_{C2X}$ $(X = l)$ will determine to what extent Fickian kinetics can ultimately be approached (and hence how important the overall deviation from Fickian kinetics will be) in the particular absorption experiment under consideration. (For $l \rightarrow \infty$, always on the assumption that the experiment is continued to $X \rightarrow l$, the initial deviation from Fickian kinetics will obviously pale into insignificance).

The difference between using the (properly defined) NF modulus/Deborah number or the "transition time" $\tau_1 = D_2/v^2$ claimed by SR to be more fundamental, appears to be essentially semantic. According to the latter terminology, the conditions for case II or diffusion-controlled penetration are given by $t/\tau_1 \rightarrow 0$ and $t/\tau_1 \rightarrow \infty$ respectively (with a "cross-over" point at $t/\tau_1 \sim 1$). However, substitution for τ_1 as above and for $t(=X/v)$ shows that $t/\tau_1 \equiv vX/D_2 \equiv \alpha_{C2X}$.

Application to Experimental Data

The experimental protocols most commonly used in *systematic* studies of the kinetics of micromolecular sorption in polymer films involve series of (i) "interval" or (ii) "integral" experiments. In a series of N interval runs, each individual run j extends over a relatively small concentration increment $\Delta C_j = |C_{Fj} - C_{Ij}|$ and the final concentration attained typically serves as the initial concentration for the next run $((C_{Fj} = C_{Ij+1})$. A series of absorption (desorption) runs commonly begins with $C_{I1} = 0$ $(C_{I1} = C_{max})$ and ends with $C_{FN} = C_{max}$ $(C_{FN} = 0)$.

In a series of N integral absorption (desorption) runs, all individual runs typically begin from (end at) the same initial (final) concentration C_{I1} (C_{FN}), which is most commonly zero, and end at (begin from) progressively increasing concentrations C_{Fj} (C_{Ij}) up to C_{max}. Thus, series of interval and integral absorption (desorption) runs may have the first (last) run in common.

Such systematic studies of sorption kinetics in glassy polymer−organic vapor systems soon brought to light general characteristic patterns of NF behavior, which are briefly described below.

Interval NF Absorption Kinetics. Series of interval experiments involving absorption in amorphous glassy polymer films, extending from $C_{I1} = 0$ to a final C_{IN} sufficiently high to attain the rubbery state, were found to be characterized by Q_t vs $t^{1/2}$ plots, which generally conformed to the pattern:[8,51]

S-shaped → pseudo-Fickian → two-stage → S-shaped or pseudo-Fickian → Fickian

(The term "pseudo-Fickian" was used by Fujita et al.[8,51] to denote cases where the Q_t vs $t^{1/2}$ plot is not visibly S-shaped but some other deviation from Fickian kinetics is discernible. These authors also reported that the above pattern is basically applicable to semicrystalline polymer films as well, except for the fact that the films studied by them became too tacky to maintain their

mechanical integrity before a final transition to Fickian kinetics could be observed).

Interpretation of these observations has been attempted in terms of the TDS modeling approach.[8,20,52,53] This seems quite reasonable, in view of the ability of this approach to account for two-stage absorption, which occupies a central position in the above pattern of behavior. Indeed, the transition from two-stage to S-shaped (and ultimately Fickian) Q_t vs $t^{1/2}$ curves at the high concentration end, can be given a straightforward and physically plausible explanation in terms of a progressive increase in $\alpha_R = l^2\beta(C)/D(C)$, resulting from the much steeper tendency of β to increase with rising C as the rubbery state is approached. This leads to progressive collapse of the two-stage absorption curve (characterized by $\alpha_R \ll 1$) to the S-shaped one ($\alpha_R \sim 1$) and ultimately to the Fickian one ($\alpha_R \rightarrow \infty$).

However, interpretation of the transition from the S-shaped to the two-stage regime at low C_I, on this basis, is less straightforward. Additional model assumptions are required, about the appropriateness of which there has been no general agreement. Thus, Fujita and Kishimoto assumed that what has been termed here "elastic swelling" is in reality "fast viscous swelling", governed by a relaxation frequency β' (much higher than β), which is also an increasing function of concentration.[8] One may then presume that $\alpha'_R = l^2\beta'/D \sim 1$ at the low C_I end of the series, where S-shaped curves are observed (and appear to attain equilibrium, because $l^2\beta/D$ is still too low for the main relaxation governed by β to become manifest on a reasonable experimental time scale); and $\alpha'_R \rightarrow \infty$ at some concentration between the regions of pseudo-Fickian and two-stage kinetics.

An alternative view is that the S-shaped curves at low C are relaxation controlled,[20,54] i.e., they may be regarded as the second stage of a two-stage absorption process lacking a visible first stage. This theory becomes more credible for systems exhibiting characteristics similar to those of the cellulose acetate−acetone one studied by Bagley and Long[54] (BL), who first took up this line of argument. In this system, β is strongly dependent on the magnitude of ΔC but tends to be insensitive to that of C (see below). For the values of ΔC used in BL's interval sorption runs, the absorption rates, which characterize the S-shaped and second-stage Q_t vs $t^{1/2}$ curves, are indeed quite similar (as illustrated in Figure 1 below).

It appeared to us that application of systematic kinetic analysis of the type presented in the preceding section was likely to yield important new insight into the nature of the NF sorption behavior discussed above and that the system originally studied by BL would be a good choice for this purpose.

These considerations led to the initiation of our detailed experimental investigation of the sorption of acetone vapor by mercury-cast CA films (and the resulting longitudinal swelling of the latter), which has already been referred to in the introductory section. For a full account of the experimental details and of the results obtained concerning diverse facets of equilibrium and kinetic behavior, including successful identification and general interpretation of NF kinetic features, the reader should consult refs 3 and 4. Here, the latter aspect of this work is developed further, by reviewing and (with the aid of substantial additional experimental data) amplifying the evidence concerning the physical nature of various NF kinetic features and by discussing

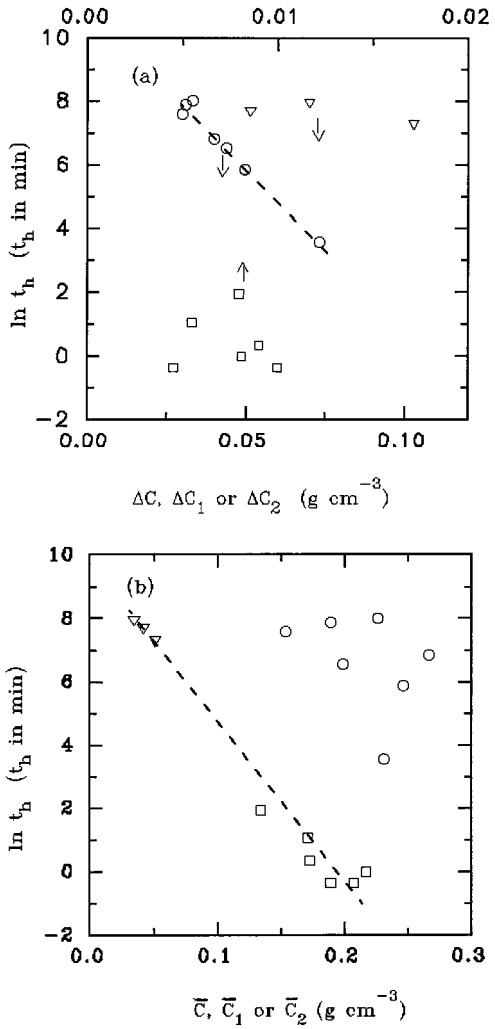

Figure 1. Observed dependence of the half-lives (t_h) of absorption Q_t vs $t^{1/2}$ curves (or portions thereof) on (a) the relevant concentration interval or (b) the relevant mean concentration: ▽, t_{hs} (low-concentration, S-shaped curves) vs (a) $\Delta C = C_F - C_I$ or (b) $\bar{C} = 0.5(C_I + C_F)$; □, t_{h1} (first stage of two-stage curves) vs (a) $\Delta C_1 = C_q - C_I$ or (b) $\bar{C}_1 = 0.5(C_I + C_q)$; ○, t_{h2} (second stage of two-stage curves) vs (a) $\Delta C_2 = C_F - C_q$ or (b) $\bar{C}_2 = 0.5(C_q + C_F)$ (see text); $2l = 59$ μm.

in detail their appearance and evolution, in the light of model predictions.

Analysis of Interval NF Absorption Kinetics in the CA−Acetone System. An important line of investigation pursued in the course of this work consisted of performing successive series of interval absorption runs on the same film specimen. Each series covered the same concentration range (namely $C_{I1} \approx 0$ to $C_{FN} = C_{max} \approx 0.3$ g cm^{-3}; C_{max} was chosen as high as possible, consistent with the need to exclude any possibility of impairment of the mechanical integrity of the film specimen in the course of these experiments), but ΔC was increased (and the number of steps N correspondingly reduced) from one series to the next (as illustrated in Figures 2−4 of ref 3). In the concentration range studied, one can observe the transition of the Q_t vs $t^{1/2}$ plot from S-shaped at low C, to two-stage at high C_I, in series characterized by low ΔC.

The fact that, as stated above, the S-shaped and second-stage absorption rates are not very different at the lowest ΔC values studied (which correspond to those used by BL), is illustrated in Figure 1a, where the relevant half-lives (i.e., the times at which $Q_t = 0.5Q_\infty$),

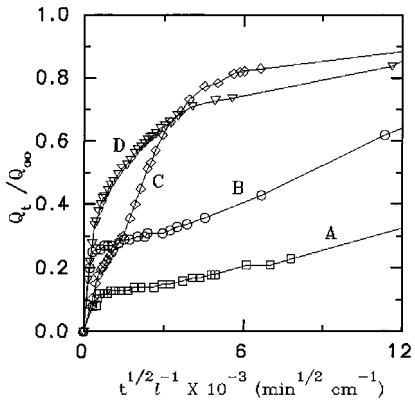

Figure 2. Examples of low-ΔC (curve A) and higher-ΔC (curve C) two-stage absorption and corresponding desorption (curves B, D respectively) behavior: $C_I = 0.20$ (A), 0.24 (B), 0.20 (C), 0.29 (D) g cm^{-3}; $\Delta C = 0.032$ (A), 0.040 (B), 0.064 (C), 0.048 (D) g cm^{-3}; $\Delta C_1 = C_q - C_I = 0.0035$ (A), 0.010 (B), 0.019 (C), − (D) g cm^{-3}; $2l = 59$ (A, B), 62 (C, D) μm.

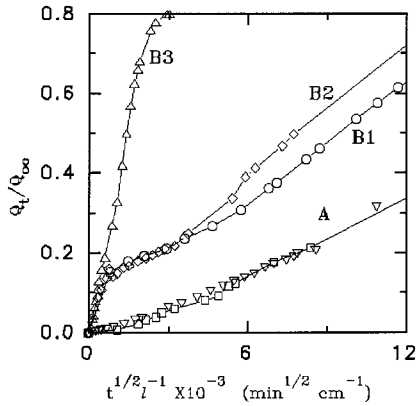

Figure 3. Film thickness dependence of typical S-shaped ($C_I \approx 0$, curves A) and two-stage ($C_I \approx 0.18$ g cm^{-3}, curves B) reduced absorption plots covering small concentration increments $\Delta C \approx 0.050$ g cm^{-3}: $2l = 43$ (○), 59 (□, ◇), or 231 (▽, △) μm.

t_{hs} (triangles) and t_{h2} (circles) respectively, are shown. However, Figure 1a also shows that, as $\Delta C_2 = C_F - C_q$ increases, t_{h2} declines rapidly; in contrast to t_{hs}, which does not vary substantially with ΔC. This observation throws strong doubt on the suggested (see above) physical similarity between second-stage and low-C_I, S-shaped absorption curves. Since $\beta \propto 1/t_{h2}$, the aforementioned behavior of t_{h2} reflects the marked positive functional dependence of β on ΔC; which leads to rapid rise of $\alpha_R = l^2\beta/D$ and hence to collapse of two-stage absorption curves (as illustrated in Figure 2) ultimately to S-shaped ones, when ΔC becomes sufficiently high. Figure 1a shows further that the half-life t_{h1} of the first stage of two-stage absorption (squares), also exhibits no significant dependence on ΔC.

On the other hand, the absence of substantial dependence of β on concentration is reflected in the lack of significant correlation between t_{h2} and $\bar{C}_2 = 0.5(C_q + C_F)$, shown in Figure 1b. In contrast to this, both t_{hs} [plotted in Figure 1b vs $\bar{C} = 0.5(C_1 + C_F)$] and t_{h1} [shown in Figure 1b as a function of $\bar{C}_1 = 0.5(C_I + C_q)$] exhibit definite negative concentration dependence; it is particularly striking that the relevant data appear to fall very nearly on the same correlation line. In accordance with what has been said about the nature of two-stage sorption in the introductory section, t_{h1} should reflect the behavior of the diffusivity (in fact, we expect $D \approx 0.049l^2/t_{h1}$).[6d] Hence, the above analysis strongly suggests that t_{hs} is also diffusion-controlled.

Conclusive evidence for the above picture is afforded by the effect of varying film thickness. As shown in ref 3 and illustrated more effectively with significant new data in Figure 3 here, increasing l produces a marked progressive shift (to the left) of the second stage of two-stage Q_t/Q_∞ vs $t^{1/2}/l$ plots, while the first stage remains essentially unaffected, thus confirming its diffusion-controlled nature. (The two stages thus tend to merge into an S-shaped curve, in line with the resulting change in α_R, which, in the example given, covered the range $\alpha_R \simeq 0.003$ for curve B1 to $\alpha_R \simeq 0.15$ for curve B3). The change in l also had no effect on low-C_I, S-shaped Q_t/Q_∞ vs $t^{1/2}/l$ plots (as illustrated by curves A in Figure 3). Hence, (following the theoretical criteria enunciated in the preceding section), the S shape of the latter plots should be interpreted in terms of DSS effects, *in the absence* of viscous relaxation phenomena.

Integral NF Absorption Kinetics. Integral NF sorption behavior is less varied (and correspondingly less informative) than that of interval sorption but can nevertheless furnish useful additional mechanistic information and may also exhibit interesting kinetic features (such as NF feature 5) not observed in normal interval sorption experiments. It is typically characterized by Q_t vs $t^{1/2}$ plots exhibiting NF feature 1. A tendency of increasing deviation from Fickian kinetics with rising ΔC is commonly seen, resulting in a more pronounced S shape of the absorption plot.[55] Replotting the latter on a t scale may yield NF feature 5 (case II kinetics)[12] or feature 6 (super case II kinetics).[56] Attempts have been made to quantify these observations on the basis of a power law $Q_t = \text{const} \times t^n$; wherein $n = 0.5$ for Fickian kinetics under semiinfinite medium conditions. Increasing values of $n > 0.5$ then denote increasing deviation from Fickian kinetics with $n = 1$ for case II, and $n > 1$ for super case II, kinetics (note, incidentally, that "subdiffusive regimes" characterized by $n < 0.5$ are also possible, e.g., for diffusion in fractal diffusion media).[57]

Although the above simplistic scheme of data analysis is undoubtedly useful for purely descriptive purposes, its validity is limited by the fact that (with the exception of $n = 1$ for the case II regime) there is no fundamental reason for expecting NF sorption kinetics of any kind to conform to a power law. Reported values of n are thus subject to uncertainty with regard to the degree of conformity of the relevant absorption data to the assumed power law. This is particularly serious in the case of $n > 1$[56] (as is illustrated also below); such values may, in fact, be viewed as indicating the appearance of NF feature 6 but can hardly be assigned any further quantitative significance. On the other hand, based on the consideration that $n = 1$ represents an extreme form of viscous relaxation-controlled kinetics, it is often taken for granted that values of $0.5 < n < 1$ may be taken as evidence of (correspondingly more moderately) relaxation-controlled kinetic regimes.[12,26,56] Here, one should be careful not to lose sight of the fact that purely DSS-induced deviations from Fickian kinetics may also exhibit reasonable conformity to the above power law with similar n values, as is illustrated below.

Analysis of Integral NF Absorption Kinetics in the CA−Acetone System. In our own integral sorption results relating to the cellulose acetate−acetone system (in the range $C \approx 0$ to $C_{max} \approx 0.3$ g cm^{-3}), apart from

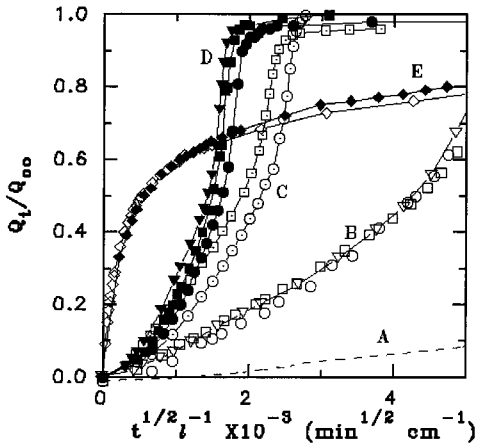

Figure 4. Concentration and film thickness dependence of reduced integral absorption kinetic plots: $C_I \approx 0$; $\Delta C = 0.050$ (curve A, identical with curves A of Figure 3), 0.17 (curves B), 0.22 (curves C), 0.31 (curves D) g cm^{-3}; $2l = 42$ (circles, curves B1, C1, D1), 59 (squares, curve D2), 62 (squares, curves B2, C2), and 112 (triangles, curves B3, D3) μm. Examples of corresponding desorption plots (limited to two for clarity) are also given (curves E): $C_F \approx 0$; $\Delta C = 0.31$ g cm^{-3}; $2l = 42$ (◆, curve E1) or 112 (◇, curve E2) μm.

NF feature 1, the appearance of features 3, 4, and 6 was also noted under various conditions.[3] Here, we first complete the picture by establishing the presence of NF feature 5 and then proceed to follow and discuss in detail the development of all these NF features, on the basis of a more complete set of data.

Absence of NF feature 3 (i.e., absence of discrepancies between Q_t/Q_∞ vs $t^{1/2}/l$ plots pertaining to different l) has already been demonstrated in Figure 3 for absorption experiments extending from $C_I \approx 0$ to $C_F \approx 0.05$ g cm^{-3} (represented by curve A in both Figure 3 and Figure 4). Curves B in Figure 4 reveal no substantial deviation from this behavior for C_F values extending as far as the middle ($C_F \approx 0.17$ g cm^{-3}) of the total concentration range studied. NF feature 3, however, unmistakably appears at still higher C_F, in the form of a regularly increasing shift to the left of the Q_t/Q_∞ vs $t^{1/2}/l$ plot with rising l, as illustrated by curves C and D in Figure 4. Thus, in the upper half of the C_F range studied, viscous relaxation effects definitely become important.

It is therefore, interesting to see to what extent the extended (viscoelastic) DSS model[18,31,32] referred to above can provide a theoretical interpretation encompassing the whole range of NF behavior displayed in Figure 4. The magnitude of the deviation from Fickian absorption kinetics is essentially determined by the rate at which the DSS build up and decay. The DSS of critical importance here is the compressive stress imposed by the rigid unswollen core on the softened swelling outer layers of the polymer film, which tends to prevent swelling of the latter in the longitudinal directions (while the corresponding tensile DSS exercised by the outer swelling layers on the unswollen core may also be a significant contributing factor; see Figure 4 of ref 31). As a result of this, uptake of penetrant by the outer layers is partially suppressed. The compressive stress in question is progressively relieved, as the penetrant spreads out across the film (as illustrated in Figure 4 of ref 31). The rate of penetrant uptake is thereby progressively enhanced, thus giving rise to the S-shaped Q_t vs $t^{1/2}$ absorption curves seen in the lower C_F region. According to the viscoelastic DSS modeling

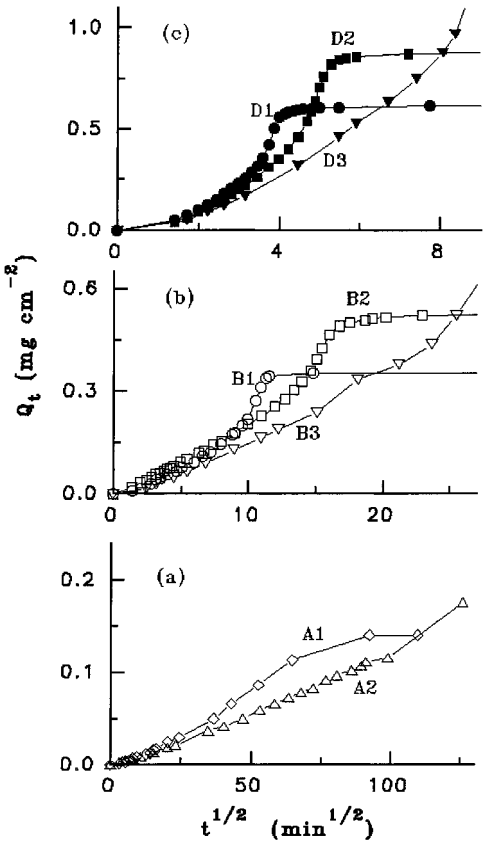

Figure 5. Illustration of NF feature 4 using absorption data for $C_I \approx 0$ and (a) $C_F = 0.05$ g cm^{-3} (curves A), (b) $C_F = 0.17$ g cm^{-3} (curves B), and (c) $C_F = 0.31$ g cm^{-3} (curves D); $2l = 42$ (curves B1, D1), 59 (curves Al, D2), 62 (curve B2), 112 (curves B3,D3), and 231 (curve A2) μm.

approach, the aforementioned diffusion-controlled effect is further intensified by that of viscous stress relaxation, which is governed by the stress relaxation modulus $\alpha_s = l^2\beta_s/D$. Within the framework of the dimensionless Q_t/Q_∞ vs $t^{1/2}/l$ plot, increasing α_s implies enhanced rate of stress relaxation relative to diffusion; hence, the shift of the aforesaid plot to the left with rising l (shown in Figure 4) is duly predicted. This process soon attains a limit as $\alpha_s \rightarrow \infty$.

The data of Figure 4 are suitably replotted in Figures 5 and 6 to demonstrate the development of NF features 4 and 6, respectively. In particular, it should be noted that NF feature 4 remains as prominent well above (Figure 5c), as it can be near (Figure 5b) the threshold of appearance of NF feature 3. On the other hand, Figure 6 shows that NF feature 6 is absent from curve A; it first appears in curve B and becomes progressively more prominent with rising C_F (curves C and D). These findings support the view that DSS effects remain strong in the high C_F region.

NF features 4 and 6 are also manifestations of the aforementioned increase in absorption rate resulting from relief of the compressive DSS imposed on the outer swollen layers of the film by the more rigid core (decay of the stress in question is obviously favored increasingly, as the core is progressively penetrated, and hence increasingly swollen as well as softened, during the later stages of the absorption process). In particular, NF feature 4 reflects the fact that compressive stress relief occurs earlier in real time when l is lower.[2] This is expected to be true quite generally, in keeping with the fact that NF feature 4 has been detected

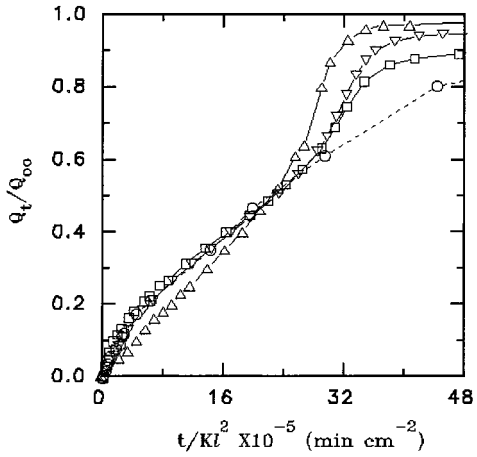

Figure 6. Illustration of the development of NF feature 6 (super-case II kinetics), using absorption data scaled to coincide at $Q_t/Q_\infty \approx 0.5$, to facilitate comparison: $C_I \approx 0$; $C_F =$ 0.05 (○, curve A), 0.17 (□, curve B), 0.22 (▽, curve C), and 0.31 (△, curve D) g cm^{-3}; K = 68.20 (A), 7.75 (B), 1.62 (C), 1 (D); $2l$ = 59 μm.

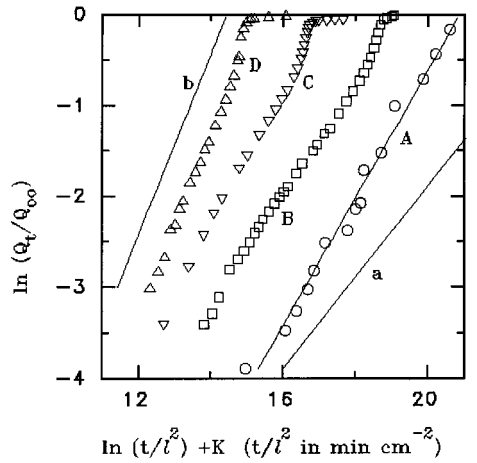

Figure 7. Replot of data of Figure 6 on a log−log basis with the same symbols. Lines a and b represent slopes of $n = 0.5$ and n = l, respectively. $K = 0$ (D), 1 (A, C), and 1.5 (B).

here at all C_F studied (cf. Figure 5a−c).

On the other hand, the appearance of NF feature 6 is dependent on a sufficiently abrupt completion of the rigid core attrition process (resulting in a correspondingly pronounced acceleration of penetrant uptake), which is obviously favored by a steep penetration front. This is in keeping with the behavior displayed in Figure 6, since the relevant penetration fronts are expected to become steeper with increasing C_F (due to the more pronounced variation of D as a function of C).

In the range of $Q_t/Q_\infty \leq 0.5$ (which should correspond roughly to the semiinfinite medium regime), Figure 6 reveals relatively little differentiation in kinetic behavior with increasing C_F, except at $C_F = C_{max}$, where a substantial shift of the Q_t vs t plot to near linearity can be seen. Replotting the data of Figure 6 on a log−log basis in Figure 7 confirms the close approach of curve D to a case II regime, on one hand, and reveals significant differences in kinetic behavior (not easily discernible in Figure 6) among curves A−C, on the other hand. These differences cannot, however, be described simply in terms of different values of the power law exponent n. In fact, curves B and C are examples of NF absorption data exhibiting poor conformity to the power law (even under semiinfinite medium conditions). On

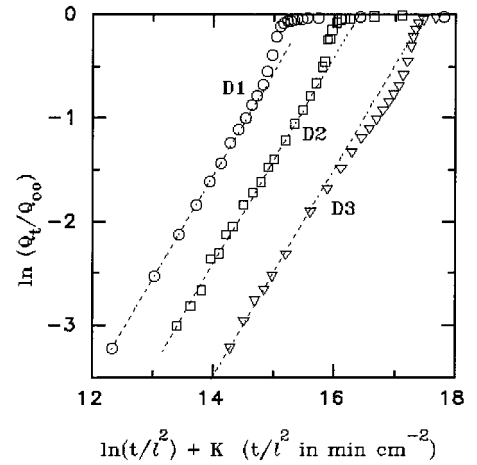

Figure 8. Effect of film thickness on the appearance of NF feature 5 (case II kinetics) for $C_I \approx 0$, $C_F = 0.31$ g cm^{-3}: $2l$ = 42 (curve D1), 59 (curve D2, identical with curve D in Figure 7), and 112 (curve D3) μm; $K = 0$ (D1), 1 (D2), and 2.5 (D3). The lines represent slope $n = 1$.

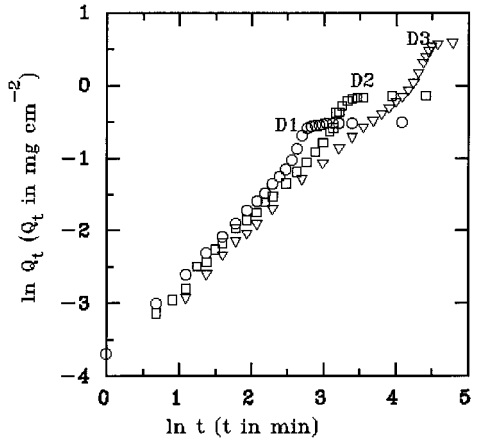

Figure 9. Replot of the data of Figure 8 with the same symbols, to illustrate the degree of coincidence observed in the semiinfinite medium regime.

the other hand, curve A provides a good practical illustration of our earlier statement that DSS− induced deviations from Fickian kinetics, in the absence of viscous relaxation effects, may also exhibit reasonable conformity to the power law with $0.5 < n < 1$ (curve A yields $n = 0.71$).

In the preceding section, attention was drawn to the capability of the viscoelastic DSS model to predict case II kinetics and the requisite conditions for this were specified. Here, one may reasonably presume that the concentration range encompassed by the experiment with $C_F = C_{max}$ is sufficiently wide to ensure validity of two of these conditions, namely $\beta_s(C_F)/\beta_s(0) \gg 1$ and $D(C_F)/D(0) \gg 1$. The prevalence of a case II regime then hinges on the applicability of the remaining condition $l^2\beta_s(0)/D(C_F) \ll 1$, which is obviously favored by low l values. Figure 8 shows that variation of l in practice has the predicted effect. Curves D1 ($2l = 42$ μm) show good conformity to case II kinetics in the $Q_t/Q_\infty < 0.5$ region, while curves D3 ($2l = 112$ μm) deviate clearly therefrom.

The data of Figure 8 are replotted in Figure 9 in terms of Q_t and t, to put in evidence certain minor differences (not easily discernible in Figure 5) in the rate of penetration into films of different thickness, at times sufficiently short to ensure validity of the semiinfinite

medium regime in the thinnest film. In view of the fact that identification of NF kinetic feature 3 presupposes coincident Q_t curves under the above conditions, it is important to point out that the aforementioned discrepancies are of a magnitude that might mask a marginal appearance of NF feature 3 in curves B of Figure 4 but could hardly affect the results relating to curves A, C, and D therein. The aforesaid variation of Q_t with l is not always as regular as indicated in Figure 9, although there seems to be a consistent difference between the thickest film and the thinner ones; which could be due to thickness dependence of the magnitude of the relevant DSS or of the intrinsic diffusion properties of the polymer film. Evidence concerning the latter possibility is provided by the fact that even casting on mercury, followed by extensive annealing treatment,[3] does not seem to produce perfectly isotropic films; a small but significant tendency for in-plane macromolecular orientation (which decreases with increasing thickness) persists, and relaxes only extremely slowly during subsequent aging.[4] In accord with the findings of Dreschel et al.,[9] this should make penetrant uptake by the thick films slower. Furthermore, despite due care to subject all films to identical handling, the history of thin and thick films necessarily differs, simply by virtue of the fact that experiments with the latter must last longer.

NF Desorption Kinetics. In the desorption mode, NF behavior tends to be both less varied and less easily detectable. Thus, on one hand, similar desorption curves (cf. curve D of Figure 2 and curves E of Figure 4) may be found in cases where the corresponding NF absorption behavior (cf. curve C of Figure 2 and curves D of Figure 4) is quite different (see ref 56 for another pertinent example). On the other hand, close similarity in shape between Fickian and NF desorption curves is commonly observed. Accordingly, the diagnostic value of the latter curves is usually largely limited to their inclusion in NF kinetic feature 1.

Model calculations confirm the above picture, particularly in the case of DSS-induced NF behavior.[31,32] However, the presence of viscous relaxation phenomena should be detectable via NF feature 3 in the desorption mode too. Curves E in Figure 4 show that this is, indeed, true, although the magnitude of the effect is considerably smaller than in the corresponding absorption data (cf. curves D of Figure 4). On the other hand, the TDS model predicts that the desorption curve should converge to the absorption one (whether S-shaped or two-stage), as the concentration dependence of D and β diminishes. Accordingly, significant changes in the shape of the desorption curve may be expected as $\Delta C \rightarrow 0$. Figure 2 shows that this, indeed, happens. Reduction of ΔC leads, on one hand, to diminution of β and hence of α_R, thus enhancing the two-stage character of the absorption plot (curve C → A); on the other hand, the fully upward convex desorption plot is converted to two-stage (curve D → B). This behavior, incidentally, contrasts sharply with what would be expected, if the interpretation of two-stage absorption in terms of a case II mechanism proposed in ref 48 (see previous section) was tenable.

Sorption−Longitudinal Swelling (S−LS) Kinetic Correlation. The basic mechanism of DSS-induced NF absorption, referred to in the preceding subsection, involves initial restriction of penetrant uptake by suppression of longitudinal swelling and, should, therefore,

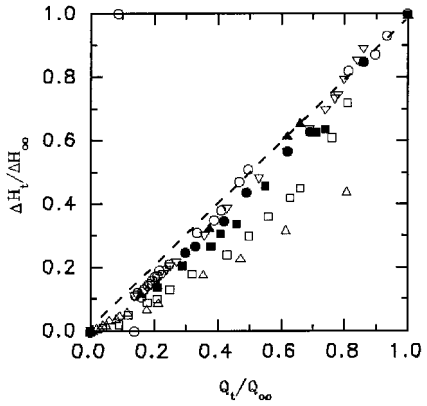

Figure 10. Sorption−longitudinal swelling kinetic correlations pertinent to the interval absorption experiments represented by curves A (△), B1 (▽), B2 (○), and B3 (□) of Figure 3. Examples of the corresponding correlations in the desorption mode (filled symbols) are also given.

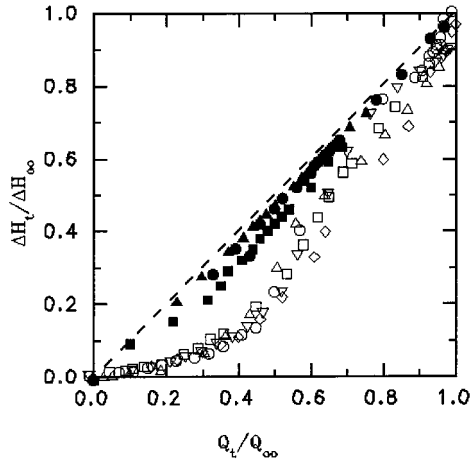

Figure 11. Examples of sorption-longitudinal swelling kinetic correlations pertinent to the integral absorption experiments represented by curves B1 (□), C1 (▽), D1 (○), D2 (◇), and D3 (△) of Figure 4. Examples of the corresponding correlations in the desorption mode (filled symbols) are also given.

be characterized by negative deviation from linearity of the dimensionless S−LS kinetic correlation plot $\Delta H_t/\Delta H_\infty$ vs Q_t/Q_∞ (see preceding section), especially during the early stages of the experiment. The extent and temporal evolution of the deviation in question should reflect the magnitude and decay of the compressive DSS on the outer film layers; so, the observed behavior is expected to depend on such factors as the magnitude of ΔC and the viscoelastic properties of the polymer, as well as their dependence on penetrant concentration.

Figures 10 and 11 show that the S−LS correlation plots, corresponding to the interval and integral absorption data presented above in Figures 3 and 4, respectively, are consistent with the interpretation given to these data. In particular, marked negative deviations from linearity are found (see Figure 11 and curve A in Figure 10) in all cases (namely curve A in Figure 3 and curves A−D in Figure 4) where NF absorption kinetic analysis points to substantial DSS effects. On the other hand, there is little deviation from linearity (see curve B1 in Figure 10) in the case of two-stage absorption characterized by a low α_R (curve B1 of Figure 3 where $\alpha_R \approx 0.003$), where quasiequilibrium is attained at an early stage and no significant concentration gradients (and hence no appreciable DSS) are expected thereafter. Characteristically, a significant deviation from linearity

appears (curve B3 of Figure 10) when l is increased sufficiently for α_R to approach unity. In this case, the two stages have merged to a large extent (see curve B3 of Figure 3 where $\alpha_R \approx 0.15$) and substantial concentration gradients (and hence appreciable DSS) are expected to persist over most of the Q_t/Q_∞ range.

The plots of Figure 11 reflect the expected initial strong suppression of LS. The lag between penetrant uptake and LS appears to attain a maximum at $Q_t/Q_\infty \sim 0.5$ and to decline sharply in the region $Q_t/Q_\infty \sim 0.6-0.7$, corresponding to the end of the semiinfinite medium regime and to the presence of NF feature 6, respectively. The effect of changes in C_F (and secondarily in l) is relatively small and difficult to establish, because of the limited reproducibility of the LS data, which is primarily responsible for the scatter of the points of Figure 11.[4] In this connection, one should bear in mind that increasing C_F entails decline of the linear elastic modulus as well as depression of the limit of linear elasticity of the polymer.[4] Both these effects tend to attenuate the magnitude of the resulting DSS.

The representative examples of desorption−longitudinal contraction plots, included in Figures 10 and 11, illustrate the fact that only small (and usually negative) deviations from linearity were found under all conditions studied. This result, which might appear strange at first sight, constitutes a useful criterion of nonlinear elastic or viscoelastic behavior.[33] This and other aspects of the mechanical and swelling behavior of the CA−acetone system are discussed in greater detail in ref 4.

Conclusion

The present paper confirms and amplifies our previous demonstration[3] that systematic kinetic analysis and model interpretation of weight gain (and loss) data (which constitute by far the largest body of available data) can yield very significant insight into the physics underlying various aspects of the NF sorption behavior of polymer film−organic vapor systems. The main general outcome of this analysis is that the said NF behavior cannot be fully understood without invoking *both* viscous relaxation and (the so far largely ignored) DSS effects.

More specifically, it has been shown that, in the CA−acetone system, the latter effects are exclusively responsible for the appearance of NF feature 1 at the low-concentration end of series of both interval and integral absorption runs. Viscous relaxation effects were found to appear only at higher concentration, in the form of two-stage sorption and NF feature 3, respectively. These findings, in conjunction with similar results recently derived from a very different system, namely poly(methyl methacrylate)−methyl acetate,[58] point toward fundamental revision of the interpretation (at present based wholly on viscous relaxation effects) of NF interval and integral absorption behavior of polymer-vapor systems *in general*.

On the other hand, the possibility of interpreting observed NF sorption behavior, with any generality, without invoking viscous relaxation effects, seem to us much more restricted than suggested by SR.

For more detailed interpretation of NF sorption data and in the absence of a rigorous comprehensive treatment (highly desirable in principle,[59] but too complex to formulate in practice, except in the simplest case[60] which is not relevant here), we have found that the separate VVR and DSS modeling approaches initiated by Crank[2] still offer what appears to be the best combination of simplicity and usefulness. A noteworthy result in this respect is the present demonstration that the full range of integral sorption behavior of the CA−acetone system, which includes NF features 1 and 3−6 can be understood in terms of the viscoelastic DSS model approach.

List of Acronyms and Symbols

NF = non-Fickian (sorption kinetics)
DSS = differential swelling stress (effect or modeling approach)
VVR = viscous volume relaxation (modeling approach)
VR = viscous relaxation (effect)
CA = cellulose acetate
BL = Bagley and Long[54]
SR = Samus and Rossi[5]
LS = longitudinal swelling
S−LS = sorption−longitudinal swelling (correlation)
TDS = time-dependent solubility
TDD = time-dependent diffusivity
DwC = diffusion with convection (modeling approach)
C = concentration of sorbed penetrant
a = penetrant activity
C_I (a_I) = initial (uniform) concentration (activity) for a sorption experiment
C_F (a_F) = final (uniform) concentration (activity) for a sorption experiment
Q_t (Q_∞) = amount of penetrant absorbed or desorbed at time t (final equilibrium)
l = half-thickness of polymer film
D = diffusion coefficient
$S = C/a$ = solubility coefficient
α = "NF modulus" (introduced by Crank;[2] reciprocal of "Deborah number" introduced by Vrentas et al.[29])
τ = relaxation time
β = volume relaxation frequency (reciprocal of relaxation time τ)
β_s = stress relaxation frequency
$\Delta C = C_F - C_I$
C_1 (C_2) = concentration during the first (second) stage of two-stage sorption
C_q = concentration at the quasiequilibrium plateau marking the end of the first stage of two-stage sorption
ΔH_t (ΔH_∞) = change in film length, during a sorption experiment, at time t (final equilibrium)
v = convection velocity
n = exponent of the empirical power law $Q_t = \text{const}\ t^n$
C_{max} = upper end of the concentration range covered by a series of sorption experiment

References and Notes

(1) Crank, J.; Park, G. S. *Trans. Faraday Soc.* **1951**, *47*, 1072.
(2) Crank, J. J. *Polym. Sci.* **1953**, *11*, 151.
(3) Sanopoulou, M.; Roussis, P. P.; Petropoulos, J. H. J. *Polym. Sci., Part B: Polym. Phys.* **1995**, *33*, 993.
(4) Sanopoulou, M.; Roussis, P. P.; Petropoulos, J. H. J. *Polym. Sci., Part B: Polym. Phys.* **1995**, *33*, 2125.
(5) Samus, M. A.; Rossi, G. *Macromolecules* **1996**, *29*, 2275.
(6) Crank, J. *The Mathematics of Diffusion*, 2nd ed.; Oxford University Press: London, 1975: (a) Chapter 4; (b) Chapter 11; (c) Chapter 13; (d) Chapter 10.
(7) Long, F. A.; Richman, D. J. *Am. Chem. Soc.* **1960**, *82*, 513.
(8) Fujita, H. *Fortschr. Hochpolym. Forsch.* **1961**, *3*, 1.
(9) Dreschel, P.; Hoard, J. L.; Long, F. A. J. *Polym. Sci.* **1953**, *10*, 241.
(10) Jacques, C. H. M.; Hopfenberg, H. B.; Stannett, V. In *Permeability of Plastic Films and Coatings to Gases, Vapors and Liquids*; Hopfenberg, H. B., Ed.; Plenum: New York, 1974; p 73.
(11) Alfrey, T.; Gurnee, E. F.; Lloyd, W. G. *J. Polym. Sci., Part C* **1966**, *12*, 249.
(12) Hopfenberg, H. B.; Holley, R. H.; Stannett, V. *Polym. Eng. Sci.* **1969**, *9*, 242.
(13) Frisch, H. L. *J. Chem. Phys.* **1964**, *41*, 3679.

(14) Newns, A. C. *Trans. Faraday Soc.* **1956**, *52*, 1533.
(15) Petropoulos, J. H.; Roussis, P. P. *J. Chem. Phys.* **1967**, *47*, 1491.
(16) Petropoulos, J. H.; Roussis, P. P. *J. Polym. Sci., Part C* **1969**, *22*, 917.
(17) Petropoulos, J. H.; Roussis, P. P. In *Organic Solid State Chemistry*; Adler, G., Ed.; Gordon and Breach: London, 1969; p 43.
(18) Petropoulos, J. H.; Roussis, P. P. In *Permeability of Plastic Films and Coatings to Gases, Vapors and Liquids*; Hopfenberg, H. B., Ed.; Plenum: New York, 1974; p 219.
(19) Petropoulos, J. H. *J. Polym. Sci., Polym. Phys. Ed.* **1984**, *22*, 1885.
(20) Durning, C. J. *J. Polym. Sci., Polym. Phys. Ed.* **1985**, *23*, 1831.
(21) Durning, C. J.; Tabor, M. *Macromolecules* **1986**, *19*, 2220.
(22) Cohen, D. S. *J. Polym. Sci., Polym. Phys. Ed.* **1983**, *21*, 2057; **1984**, *22*, 1001.
(23) Joshi, S.; Astarita, G. *Polymer* **1979**, *20*, 455.
(24) Wu, J. C.; Peppas, N. A. *J. Polym. Sci., Part B: Polym. Phys.* **1993**, *31*, 1503.
(25) Huang, S. J.; Durning, C. J. J. *Polym. Sci., Part B: Polym. Phys.* **1997**, *35*, 2103.
(26) Kim, D. J.; Caruthers, J. M.; Peppas, N. A. *Chem. Eng. Sci.* **1996**, *51*, 4827.
(27) Thomas, N. L.; Windle, A. H. *Polymer* **1982**, *23*, 529.
(28) Petropoulos, J. H. In *Advances in Membrane Phenomena and Processes*; Mika, A. M., Winnicki, T. Z., Eds.; Wroclaw Technical University Press: Wroclaw, Poland, 1989; p 45.
(29) Vrentas, J. S.; Jarzebski, C. M.; Duda, J. L. *AIChE J.* **1975**, *21*, 894.
(30) Tamura, M.; Yamada, K.; Odani, J. *Rep. Prog. Polym. Phys., Jpn.* **1963**, *6*, 163.
(31) Petropoulos, J. H.; Roussis, P. P. *J. Membr. Sci.* **1978**, *3*, 343.
(32) Petropoulos, J. H. *J. Membr. Sci.* **1984**, *18*, 37.
(33) Petropoulos, J. H. *J. Membr. Sci.* **1984**, *17*, 233.
(34) Petropoulos, J. H. *J. Polym. Sci., Polym. Phys. Ed.* **1984**, *22*, 183.
(35) Kim, M.; Neogi, P. J. *Appl. Polym. Sci.* **1984**, *29*, 731.
(36) Neogi, P.; Kim, M.; Yun Yang *AIChE. J.* **1986**, *32*, 1146.
(37) Ware, R. A.; Cohen, C. *J. Appl. Polym. Sci.* **1980**, *25*, 717.
(38) Gostoli, C.; Sarti, G. C. *Polym. Eng. Sci.* **1982**, *22*, 1015; *Chem. Eng. Commun.* **1983**, *21*, 67.
(39) Fu, T. Z.; Durning, C. J.; Tong, H. M. *J. Appl. Polym. Sci.* **1991**, *43*, 709.
(40) Fang, S. M.; Stern, S. A.; Frisch, H. L. *Chem. Eng. Sci.* **1975**, *30*, 773.
(41) Sanopoulou, M.; Petropoulos, J. H. *Polymer* **1997**, *38*, 5761.
(42) Hopfenberg, H. B.; Stannett, V. In *The Physics of Glassy Polymers*; Haward, R. N., Ed.; Applied Science Publ.: London, 1973: Chapter 9.
(43) Peterlin, A. *J. Polym. Sci., Part B: Polym. Lett.* **1965**, *3*, 1083.
(44) Wang, T. T.; Kwei, T. K.; Frisch, H. L. *J. Polym. Sci., Part A2* **1967**, *7*, 2019.
(45) Astarita, G.; Sarti, G. C. *Polym. Eng. Sci.* **1978**, *18*, 388.
(46) Astarita, G.; Joshi, S. *J. Membr. Sci.* **1978**, *4*, 165.
(47) Rossi, G.; Pincus, P. A.; De Gennes, P. G. *Europhys. Lett.* **1995**, *32*, 391.
(48) Kwei, T. K. *J. Polym. Sci., Part A2* **1972**, *10*, 1849.
(49) Fu, T. Z.; Durning, C. *J. AIChE J.* **1993**, *39*, 1030.
(50) Petropoulos, J. H.; Sanopoulou, M. *J. Polym. Sci., Part B: Polym. Phys.* **1988**, *26*, 1087.
(51) Kishimoto, A.; Fujita, H.; Odani, H.; Kurata, M.; Tamura, M. *J. Phys. Chem.* **1960**, *64*, 594.
(52) Mehdizadeh, S.; Durning, C. G. *AIChE J.* **1990**, *36*, 877.
(53) Billovits, G. F.; Duming, C. G. *Macromolecules* **1994**, *27*, 7630.
(54) Bagley, E.; Long, F. A. *J. Am. Chem. Soc.* **1955**, *77*, 2172.
(55) E.g.: Odani, H.; Kida, S.; Kurata, M.; Tamura, M. *Bull. Chem. Soc. Jpn.* **1961**, *34*, 571.
(56) E.g.: Holley, R. H.; Hopfenberg, H. B.; Stannett, V. *Polym. Eng. Sci.* **1970**, *10*, 376.
(57) e.g. Gouyet, J. F. In *Diffusion in Materials*; Laskar, A. L., et al., Eds.; Kluwer: Dordrecht, The Netherlands, 1990; p 155.
(58) Boom, J. P.; Sanopoulou, M. *Polymer* **2000**, *41*, 8641.
(59) Lustig, S. R.; Caruthers, J. M.; Peppas, N. A. *Chem. Eng. Sci.* **1992**, *47*, 3037.
(60) Carbonell, R. G.; Sarti, G. C. *Ind. Eng. Chem. Res.* **1990**, *29*, 1194.

MA981255O